Adenoviral Brain-Derived Neurotrophic Factor Induces Both Neostriatal and Olfactory Neuronal Recruitment from Endogenous Progenitor Cells in the Adult Forebrain

Abdellatif Benraiss, Eva Chmielnicki, Kim Lerner, Dongyon Roh, and Steven A. Goldman

Department of Neurology and Neuroscience, Cornell University Medical College, New York, New York 10021

Neural progenitor cells persist throughout the adult forebrain subependyma, and neurons generated from them respond to brain-derived neurotrophic factor (BDNF) with enhanced maturation and survival. To induce neurogenesis from endogenous progenitors, we overexpressed BDNF in the adult ventricular zone by transducing the forebrain ependyma to constitutively express BDNF. We constructed a bicistronic adenovirus bearing BDNF under cytomegalovirus (CMV) control, and humanized green fluorescent protein (hGFP) under internal ribosomal entry site (IRES) control. This AdCMV:BDNF:IRES:hGFP (AdBDNF) was injected into the lateral ventricles of adult rats, who were treated for 18 d thereafter with the mitotic marker bromodeoxyuridine (BrdU). Three weeks after injection, BDNF averaged 1 μg/gm in the CSF of AdBDNF-injected animals but was undetectable in control CSF. *In situ* hybridization demonstrated BDNF and GFP mRNA expression restricted to the ventricular wall. In AdBDNF-injected rats, the olfactory bulb exhibited a >2.4-fold increase in the number of BrdU$^+$–βIII-tubulin$^+$ neu-

rons, confirmed by confocal imaging, relative to AdNull (AdCMV:hGFP) controls. Importantly, AdBDNF-associated neuronal recruitment to the neostriatum was also noted, with the treatment-induced addition of BrdU$^+$–NeuN$^+$–βIII-tubulin$^+$ neurons to the caudate putamen. Many of these cells also expressed glutamic acid decarboxylase, cabindin-D28, and DARPP-32 (dopamine and cAMP-regulated phosphoprotein of 32 kDa), markers of medium spiny neurons of the neostriatum. These newly generated neurons survived at least 5–8 weeks after viral induction. Thus, a single injection of adenoviral BDNF substantially augmented the recruitment of new neurons into both neurogenic and non-neurogenic sites in the adult rat brain. The intraventricular delivery of, and ependymal infection by, viral vectors encoding neurotrophic agents may be a feasible strategy for inducing neurogenesis from resident progenitor cells in the adult brain.

Key words: neurotrophic factors; neurogenesis; stem cells; gene therapy; Huntington's disease; neostriatum

Neural progenitor cells persist throughout the adult forebrain subependyma and have been found in species ranging from canaries to humans (Goldman and Nottebohm, 1983; Alvarez-Buylla and Lois, 1995; Goldman et al., 1997b; Goldman and Luskin, 1998). To the extent that neurogenesis and oligoneogenesis by these endogenous progenitors may be induced or supported exogenously, these cells may provide a cellular substrate for repair in the adult CNS. In culture, adult-derived progenitors have been found to respond to mitogens, in particular epidermal growth factor (EGF) and fibroblast growth factor-2 (FGF-2), with increased division and neuronal mitogenesis (Reynolds and Weiss, 1992; Richards et al., 1992; Vescovi et al., 1993; Palmer et al., 1995). Furthermore, neurons generated from them respond to brain-derived neurotrophic factor (BDNF) with enhanced migration, maturation, and survival *in vitro* (Kirschenbaum and Goldman, 1995; Goldman et al., 1997a; Pincus et al., 1998). Similarly,

infusions of EGF and FGF-2 into the adult ventricular system stimulate mitotic gliogenesis and neurogenesis, respectively (Craig et al., 1996; Kuhn et al., 1997), whereas intraventricular infusions of BDNF can enhance neuronal migration to the olfactory bulb, rostral migratory stream (RMS), and adjacent forebrain (Zigova et al., 1998; Pencea et al., 1999). Although intriguing, these studies have been limited by the need for chronic intraventricular catheterization, with its dependence on protein availability and stability, the uncertain tissue bioavailability of intraventricularly administered proteins, and the risks of infection and catheter loss inherent in chronic ventriculostomy.

On the basis of these studies, and of their limitations in practice, we realized the need for an efficient means of delivering neurotrophic differentiation agents to the adult subependyma. Previous studies had reported that ependymal cells could express adenovirally delivered genes after intraventricular injection of virus (Bajocchi et al., 1993; Yoon et al., 1996). The high efficiency infection of, and transgene expression by, the adult ependyma suggested to us that intraventricular delivery of adenoviral vectors might be used for the sustained delivery of neurotrophins not only to the ventricular zone but also to the CSF, and hence throughout the neuroaxis. We therefore chose to use an adenoviral vector to transduce the forebrain ependymal wall to constitutively overexpress BDNF, with the goal of inducing neurogenesis from endogenous progenitor cells. We report here that infection of the adult rat ventricular lining with an adenoviral BDNF expression vector resulted in the diffuse transduction of the adult ependymal wall, with the effective subrogation of the

ependyma into a source of secreted BDNF protein to both the CSF and periventricular parenchyma. This resulted in sustained and high-level BDNF secretion by the ventricular wall and was associated with a >2.4-fold increase in the recruitment of new neurons to the olfactory bulb in the 3 weeks after viral administration. Importantly, AdCMV:BDNF:IRES:hGFP (AdBDNF) injection was also associated with the heterotopic addition of new neurons to the neostriatum, an otherwise non-neurogenic region of the adult brain. These striatal neurons matured to express antigens typical of medium spiny neurons and were found in undiminished numbers for at least 8 weeks after AdBDNF injection. Together, these results demonstrate that viral delivery of neurotrophin genes may be a viable strategy for modulating the induction, differentiation, and fate of ventricular zone progenitor cells in the adult mammalian forebrain.

MATERIALS AND METHODS

Adenovirus construction

We constructed an adenoviral vector bearing BDNF under the control of the constitutive cytomegalovirus (CMV) promoter, placed in tandem sequence with humanized green fluorescent protein (hGFP), under the control of an internal ribosomal entry site (IRES) (Morgan et al., 1992). In brief, BDNF cDNA (Regeneron Pharmaceuticals, Tarrytown, NY) was obtained in *Spe*I/*Hin*dIII. A *Hin*dIII/*Sal*I segment containing an IRES site (Morgan et al., 1992) and hGFP were taken from pTRUFIII (Levy et al., 1996). On digestion with *Spe*I/*Hin*dIII of p*BDNF*, the 1.1 kb TRUFIII *Hin*dIII/*Sal*I fragment was ligated into the adenovirus shuttle vector pCMV:SV2, digested with *Spe*I/*Sal*I. The resultant construct was designated pAdP/CMV:BDNF:IRES:hGFP. Established methods (Graham and Prevec, 1991) were then used to construct a replication-defective recombinant adenovirus via homologous recombination using the plasmid pJM17, which contains the E1A-deleted type 5 adenovirus. pAd5/CMV:BDNF:IRES:hGFP was cotransfected with pJM17 into human embryonic kidney 293 (HEK293) cells, and viral plaques developed for 2 weeks. Crude viral lysates were then used for plaque purification. Virus was propagated in HEK293 cells, purified by cesium chloride density gradient centrifugation, and stored at $-70°C$. The resultant titer of AdBDNF was between 10^{11} and 10^{12} pfu/ml; however, both AdBDNF and its AdNull (AdCMV:hGFP) control were titered to 2.5 - 10^{10} pfu/ml before use to ensure that experimental and control rats received equivalent viral loads (see below). The efficacy of AdBDNF in driving expression of BDNF was verified in HeLa cells by ELISA. In addition, the expression of GFP by each virus was confirmed at 1 and 3 weeks after viral injection both in sections of the adult ventricular wall using direct fluorescence observation and by *in situ* hybridization of both BDNF and GFP.

Cell culture and *in vitro* experiments

HeLa cells were plated at a density of $1 \times 10^{6}/25$ cm^2 in Ham's F12 with 10% FBS. After 24 hr, the cells were infected with 1, 10, or 100 multiplicities of infection (moi) of AdBDNF or AdCMV:GFP in F12 with 1% FBS. After 24 hr, serum was added to achieve a 10% concentration of FBS. After another 24 hr, the cells were washed and switched to serum-free media for 3 d. The cells and their media were then separately collected; the media was decanted to storage at $-80°C$ for later ELISA of BDNF, and the cells were collected in Ca/Mg-free HBSS–1 mM EDTA and pelleted. The cellular pellet was then resuspended in 10% FBS-containing media and subjected to viability assay; this was done to assess potential viral toxicity in these same cultures. Triplicate 50 μl aliquots of resuspended cells were diluted in trypan blue (1:1) to label dead cells; both live and dead cells were separately counted 20 min later by a hemocytometer, and their ratio was determined.

Experimental design and stereotaxic injection

Either the AdBDNF or AdNull viruses were delivered as single 3 μl injections into the lateral ventricles of seven adult rats. Both viruses were established in the same backbone and titered to 2.5×10^{10} pfu/ml before use. Using a David Kopf Instruments (Tujunga, CA) stereotactic frame, the rats were injected at the following coordinates: anteroposterior, -0.3 mm; mediolateral, $±1.2$ mm; dorsoventral, -3.6 mm (Paxinos and Watson, 1986). The rats were injected daily for 18 d thereafter with the

mitotic marker bromodeoxyuridine (BrdU) (100 mg/kg, i.p.). Control animals were injected with either AdCMV:GFP (AdNull; $n = 5$) or PBS ($n = 5$). These animals were killed on the day after the last BrdU injection (day 20). Among them, four each of the AdBDNF-, AdNull-, and PBS-injected animals were used for the quantification of BrdU$^+$ cells in the olfactory bulb, striatum, and other regions assessed; the remainder of the animals killed on day 20 were used to supplement our assessment of the CSF BDNF levels.

An additional sample of three rats was injected with AdBDNF and BrdU as noted but killed on the 35th day after the completion of BrdU treatment, on day 56 after viral injection. These rats' brains were examined solely with regards to the persistence of BrdU$^+$ neurons in the neostriatum. In all groups, daily weights were recorded beginning with the day of viral injection, through the day of when the animal was killed.

ELISA

CSF. At 20 d after viral injection, rats were injected with 0.6 ml of 65 mg/ml pentobarbital and perfused with HBSS with Mg^{2+}/Ca^{2+} (Life Technologies, Gaithersburg, MD). CSF was collected from the cisterna magna, aliquoted, and stored at $-80°C$. The BDNF in the CSF of both PBS-injected and AdNull- or AdBDNF-injected rats was quantified using a two-site ELISA (Emax Immunoassay System; Promega, Madison, WI) (Mizisin et al., 1997), the use of which we have described previously in detail (Leventhal et al., 1999) Briefly, the monoclonal anti-BDNF capture antibody did not cross-react with other members of the neurotrophin family at concentrations up to 10,000 times that used for the standard curve, whereas the reporter antibody was a biotinylated rabbit polyclonal anti-BDNF, similarly selective for BDNF. The dynamic range of the ELISA was 10–1000 pg/ml for undiluted samples; all samples were diluted in assay buffer to bring them into the linear range of the standard curve of the assay. The CSF BDNF determinations were derived from a total of seven AdBDNF-, five AdNull-, and three PBS-injected animals. Total protein levels of each CSF sample were assessed by BCA assay (Pierce).

Cells. For the supernatants of AdBDNF- and AdNull-infected HeLa cell layers, BDNF levels were reported as the average of triplicate samples

In situ *hybridization*

Probes. BDNF antisense and sense probes were generated from pSK-rBDNF, a gift of Regeneron Pharmaceuticals. The BDNF plasmid DNA was linearized with either *Bam*HI for the antisense probe or *Eco*RV for the sense control and then transcribed *in vitro* using either T7 RNA polymerase for the antisense probe or T3 RNA polymerase for the sense probe. The antisense GFP probe was generated by linearizing pGFP with *Xba*I and transcribing *in vitro* with T3 RNA polymerase. The probes were non-isotopically labeled with digoxigenin-11-UTP (Boehringer Mannheim, Mannheim, Germany).

Hybridization. A series of 15 μm cryostat sections were permeabilized with 0.3% Triton X-100 in PBS for 15 min. The sections were dehydrated in ascending alcohols, cleared with xylene, rehydrated, treated with Proteinase K (1 μg/ml) for 30 min at 37°C, and post-fixed with 4% paraformaldehyde for 5 min. To acetylate sections, slides were incubated for 30 min in 0.1 M triethanolamine buffer, pH 8.0, containing 0.25% acetic anhydride. The sections were prehybridized with 4× SSC containing 50% formamide for 1 hr and then hybridized under coverslips for 15 hr at 42°C with digoxygenin-labeled sense or antisense probes (300 ng/ml) in 40% deionized formamide, 10% dextran sulfate, 1× Denhardt's solution, 4× SSC, 10 mM dithiothreitol, and 1 mg/ml salmon sperm DNA. After hybridization, the sections were washed in 2× SSC for 5 min to remove the coverslips, washed with 50% formamide in 2× SSC for 20 min at 52°C, washed in 2× SSC, and treated with RNase A (20 μg/ml) in 2× SSC for 30 min at 37°C. After four washes in 2× SSC, the sections were washed with 0.2× SSC at 55°C for 1 hr.

Detection of digoxygenin-labeled probes. Slides were washed in Tris-buffered saline (TBS) (0.1 M Tris-HCl with 150 mM NaCl), three times for 5 min each, blocked in 0.1% Triton X-100 and 2% sheep serum for 30 min, and then incubated overnight at 4°C in alkaline phosphatase-conjugated anti-digoxygenin (1:100; Boehringer Mannheim). After washing with TBS, the sections were switched to detection buffer (100 mM Tris-HCl, pH 9.5, with 100 mM NaCl and 50 mM MgCl$_2$) for 10 min and incubated in nitroblue-tetrazolium-chloride and 5-bromo-4-chlor-indolyl-phosphate solution (Bio-Rad, Hercules, CA) with 1 mM levamisole for 2–20 hr in the dark. During color development, the reaction was

terminated by washing (three times for 5 min each) in TBS with 10 mM EDTA.

Immunohistochemistry

The animals were killed and perfusion fixed, and their brains were removed on either the 20th or 56th day after viral injection. Fixation was accomplished using 4% paraformaldehyde in 0.1 M phosphate buffer (PB), pH 7.4, with a 90 min post-fix followed by immersion and sinking in 30% sucrose in PB. All brains were cut as 15 μm sagittal sections that included the olfactory bulb and rostral migratory stream rostrally; these were stained for BrdU using immunoperoxidase detection when staining for BrdU alone or using double-immunofluorescence when staining for both BrdU and neuronal markers. Individual sections were denatured in 2N HCl for 1 hr and then stained for BrdU using rat anti-BrdU antibody at 1:200 (Harlan Sprague Dawley, Indianapolis, IN), followed serially by fluorescein-conjugated anti-rat IgG at 1:150 (Jackson ImmunoResearch, West Grove, PA). The sections were then washed and stained for the following: βIII-tubulin, using the TuJ1 monoclonal antibody (Lee et al., 1990) (a gift of Dr. A. Frankfurter, University of Virginia Medical School, Charlottesville, VA); microtubule-associated protein-2 (MAP-2), using rabbit anti-MAP-2 (Bernhardt and Matus, 1984) (Dr. S. Halpain, The Scripps Institute, La Jolla, CA); NeuN (Eriksson et al., 1998) (Chemicon, Temecula, CA); glutamic acid decarboxylase 67 (GAD67) (Sigma, St. Louis, MO); calbindin-D28K (Guan et al., 1999) (Sigma); or DARPP-32 (dopamine and cAMP-regulated phosphoprotein of 32 kDa) (Ivkovic and Ehrlich, 1999) (Dr. H. Hemmings, Cornell University Medical College, New York, NY), each as described previously (Goldman et al., 1992; Menezes and Luskin, 1994; Eriksson et al., 1998; Guan et al., 1999; Ivkovic and Ehrlich, 1999; Roy et al., 2000). All anti-mouse secondary antibodies were preabsorbed against rat IgG to avoid nonspecific staining.

Confocal imaging

In sections double-stained for BrdU together for βIII-tubulin, MAP-2, NeuN, DARPP-32, GAD67, or calbindin-D28, single BrdU$^+$ cells appeared to be double-labeled for both the neuronal antigen and BrdU were identified and evaluated by two-color confocal imaging. Using a Zeiss (Oberkochen, Germany) LSM510 confocal microscope, images were acquired in both red and green emission channels using an argon–krypton laser. The images were then viewed as stacked z-dimension images, both as series of single 0.9 μm optical sections and as merged images thereof. The z-dimension reconstructions were all observed in profile, because every BrdU$^+$ cell double-labeled with a neuronal marker was then observed orthogonally in both the vertical and horizontal planes. Only after three observers independently deemed individual cells as double-labeled, with central BrdU immunoreactivity surrounded by neuronal immunoreactivity at all observation angles in every serial optical section and in each merged and rotated composite, were the cells scored as double-labeled, newly generated neurons.

Scoring and quantification

BrdU$^+$ cell counts. Unbiased counting was used to score the number, density, and distribution of BrdU$^+$ cells in the injected brains using an optical dissector procedure (Sterio, 1984; Kuhn et al., 1997; West, 1998). To estimate the number of BrdU-labeled cells per region, we sampled 22 15 μm sections per animal for both experimentals and controls; for each, every sixth section was analyzed at 90 μm intervals. The first section of each sagittal series was chosen randomly from a total sample that was accumulated beginning with the first appearance of the olfactory cortex on cresyl violet-stained alternate sections. Typically, the sampled region included that subtended by the stereotaxic coordinates L0.3–L2.3 bilaterally. By this means, we sampled a 2 mm mediolateral segment in the sagittal plane, centered on the RMS.

Regions assessed. The absolute number of total BrdU$^+$ cells in every eighth 15 μm sagittal section was counted in each of six regions: (1) the anterior surface of the ventricular zone, (2) the olfactory subependyma of the RMS; (3) the olfactory bulb, (4) the medial septum, (5) the neostriatum, and (6) the frontal cortex overlying the corpus callosum, rostral to the perpendicular extension of the rostral-most wall of the lateral ventricle.

Imaging and scoring. In each sampled section, every BrdU$^+$ nucleus was counted in each scored region; the positions of each of these cells were entered manually into BioQuant image analysis software with its incorporated topography reconstruction package, and the results were tabulated. For each region, the results were reported as the mean number of BrdU$^+$ cells per section. In addition, for the olfactory bulb and the neostriatum,

these counts were converted into BrdU$^+$ cells per cubic millimeter after determining the surface areas and hence volumes of each scored region (Michel and Cruz-Orive, 1988). Statistical analysis was then accomplished by ANOVA, followed by *post hoc* Boneferroni *t* tests.

Striatal neuronal counts. To estimate total striatal neuronal number, we counted the number of striatal neurons in each of six age- and sex-matched rats, three of which were treated with AdBDNF and the other three with AdNull as a negative control (*n* = 3). From each, we analyzed eight 15 μm sections, representing every 32nd sequentially, thereby sampling at 480 μm intervals beginning with the first appearance of rostrocaudally oriented striatal fascicles on cresyl violet-stained alternate sections. In these cresyl violet-stained sections, the number of neurons in each striatum was counted under high magnification using morphological criteria for neuronal identity by an observer blind as to the experimental group. To this end, neurons were defined as large cells of >10 μm diameter, with pale central nuclei and central nucleoli, in an otherwise basophilic cytoplasm. To ensure the validity of these criteria, two sections from each set of eight were destained by acidified ethanol and then immunostained for calbindin. The number of calbindin-defined striatal neurons was then counted and compared with that obtained in the same section by cresyl violet. We found >98% concordance in the neuronal counts obtained using these two methods.

RESULTS

Intraventricular delivery of adenoviral CMV:hGFP restricted transgene expression to the adult ependyma and subependyma

To first assess the distribution of adenoviral transduction after a single intraventricular injection of virus, we injected adenovirus bearing the gene encoding green fluorescent protein (hGFP), placed under the control of the CMV promoter, into the lateral ventricles of four adult Sprague Dawley rats. The rats were killed either 1 or 3 weeks later, and their brains were prepared for histology. We found that, in all four rats, most ependymal and scattered subependymal cells labeled heavily to single viral injection, with virtually the entire lining of the lateral ventricle noted to express GFP after injection of 3×10^7 pfu adenovirus (3 μl of 10^{10} pfu/ml). Little parenchymal expression of GFP was noted, despite the lack of specificity of the CMV promoter, suggesting that viral penetration outside of the subependyma was minimal (Fig. 1). The restriction of transgene expression to the ventricular wall suggested that ependymal cells might be targeted selectively on spatial grounds alone, even without benefit of cell-specific promoters.

AdBDNF-infected cells expressed BDNF *in vitro*

We next sought to assess the effects of adenovirally delivered BDNF on the adult ventricular zone pool. A ΔE1 type 5 adenovirus was thus constructed to express BDNF under the control of the constitutively activated CMV promoter; the virus also included hGFP as a reporter, placed under IRES promoter control. The resultant vector, AdBDNF, was characterized first by infecting HeLa cells, which typically do not express BDNF. The production of BDNF by the infected HeLa cells was assessed as a function of time after infection, using ELISA of BDNF secreted to the culture media. BDNF release in response to AdBDNF infection was thereby compared with that of both untransfected and AdNull-infected control cells (Fig. 2*A*,*B*). Within 2 d after infection with 10 pfu/cell AdBDNF, 234 ± 54.5 ng/ml BDNF protein was measured in the culture supernatant, ~250-fold greater than the levels observed in the uninfected (0.8 ± 1.0 ng/ml) and AdNull-infected (1.0 ± 0.6 ng/ml) control cultures. Thus, AdBDNF directed high-level expression of BDNF by HeLa cells.

To ensure that transgene expression was not accomplished at the expense of cell viability, we assessed trypan blue inclusion as a function of viral dose over the range of 1–10 moi/cell and found that adenovirus-associated toxicity was minimal and statistically
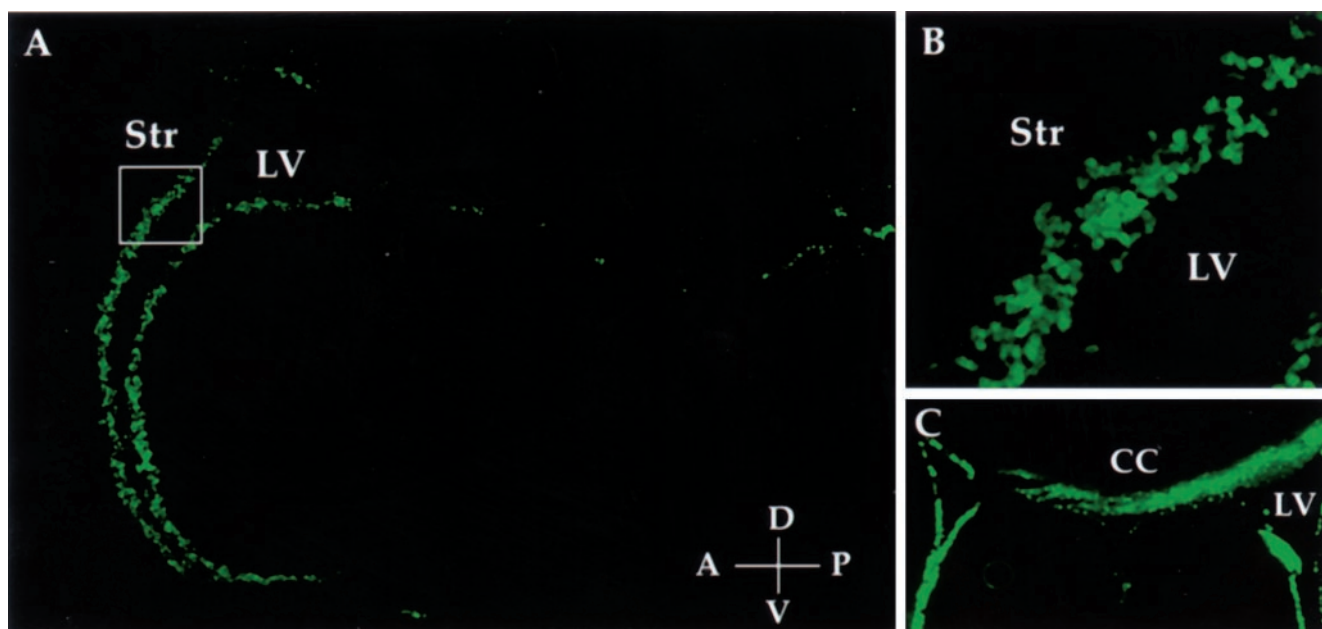
Figure 1. Ependymal restriction of intraventricular adenoviral infection. *A*, A single intraventricular injection of an adenoviral vector bearing GFP, expressed under the control of the constitutive CMV promoter, shows the widespread infection of the ventricular ependyma, bilaterally and throughout the ventricular system 1 week after viral injection. *B*, Along the striatal and septal walls, GFP expression was primarily limited to the ventricular surface, with little subependymal and no parenchymal extension. *A*, *B*, Sagittal sections. *C*, A coronal section taken at the level of the main body of the lateral ventricles again reveals GFP expression by the infected striatal and callosal ventricular surfaces. Unlike the striatal and septal walls, the callosal wall shows subependymal and some parenchymal extension of labeled cells. *Str*, Striatum; *LV*, lateral ventricle; *CC*, corpus callosum; *D*, dorsal; *V*, ventral; *A*, anterior; *P*, posterior.

insignificant over this dose range. In addition, to ensure that this dose range was no more toxic for primary brain cells than for HeLa cells, we assessed the effect of increasing viral dose on the viability of primary adult human astrocytes, obtained from temporal lobes resected from adult epileptic patients (Leventhal et al., 1999). We found that astrocytes exposed to 10 moi AdBDNF exhibited no significant increment in lethal toxicity at 48 hr after infection.

CSF levels of BDNF rose markedly after intraventricular injection of AdBDNF

To assess the level of release of BDNF protein into the CSF of AdBDNF-treated rats, a total of 14 animals were injected with AdBDNF ($n = 7$), AdNull ($n = 5$), or PBS ($n = 2$); all were subjected to cisterna magna puncture for CSF withdrawal at 3 weeks after viral infection. In the AdBDNF-injected animals, ELISA revealed that CSF BDNF levels averaged 1.07 ± 0.3 μg/gm protein (mean $\pm$ SE) when assessed 3 weeks after injection (Fig. 2*C,D*). This represented 2.02 ± 0.6 ng of BDNF per milliliter of ventricular CSF, a level within the dose range appropriate for eliciting TrkB-mediated biological effects *in vitro* (Lindsay et al., 1994). In contrast, BDNF was undetectable in both the PBS and AdCMV:GFP controls ($p = 0.025$ by ANOVA; $F_{(2,13)} = 5.24$). The absence of detectable BDNF in the AdNull-injected controls indicated that the BDNF levels achieved in the CSF of AdBDNF-treated animals was a product of the virally encoded BDNF transgene. Thus, adenoviral transduction of the adult ventricular ependyma permitted high-level delivery of BDNF to the brain and CSF, with expression that was sustained for at least 3 weeks after viral infection.

Adenoviral-transduced BDNF mRNA was restricted to the ventricular wall

In situ hybridization, using RNA probes for BDNF and hGFP, revealed that AdCMV:BDNF:IRES:GFP transduced expression of both BDNF and hGFP mRNA *in vivo*. Strikingly, BDNF and GFP mRNAs were largely restricted to the wall of the lateral ventricular system (Fig. 3). Even when assessed 3 weeks after viral injection, cells overexpressing BDNF and GFP were primarily limited to the ventricular wall, with little or no infiltration of the rostral migratory stream or bulb. Thus, at least rostrally along the anterior face of the ventricle, the infected cell pool appeared to be ependymal, with little or no direct infection of subependymal neuronal migrants. This pattern appeared to be maintained along most of the rostrocaudal extent of the ventricular system, throughout which virally transduced BDNF and GFP mRNAs were limited to the ependymal surface, except at the rostral tip of the lateral ventricles, in which scattered subependymal labeling was also noted.

AdBDNF infection of the ventricular wall increased substantially the number of new neurons in both the rostral migratory stream and olfactory bulb

To follow the generation and fates of new neurons generated from the AdBDNF-treated ventricular zone, we injected an initial cohort of rats with either AdBDNF or AdNull ($n = 4$ per group). These injections were followed with daily intraperitoneal injections of BrdU at 100 mg/kg for the next 18 d. On day 20, the animals were killed, CSF was extracted for BDNF ELISA, and the brains were fixed along with the olfactory bulbs. The brains were then sectioned and stained for BrdU in tandem with phenotype-specific markers (Fig. 4).

The effects of AdBDNF on neuronal recruitment were first assessed in the region of the rostral migratory stream, as measured posteriorly from the striatum and its ventricular wall up to, and including, the internal granular layer of the olfactory bulb. Within this region, the incidence of BrdU$^+$ cells rose from 3398 ± 346 cells/mm^3 (mean $\pm$ SE) in the control animals to 8288 ± 1199
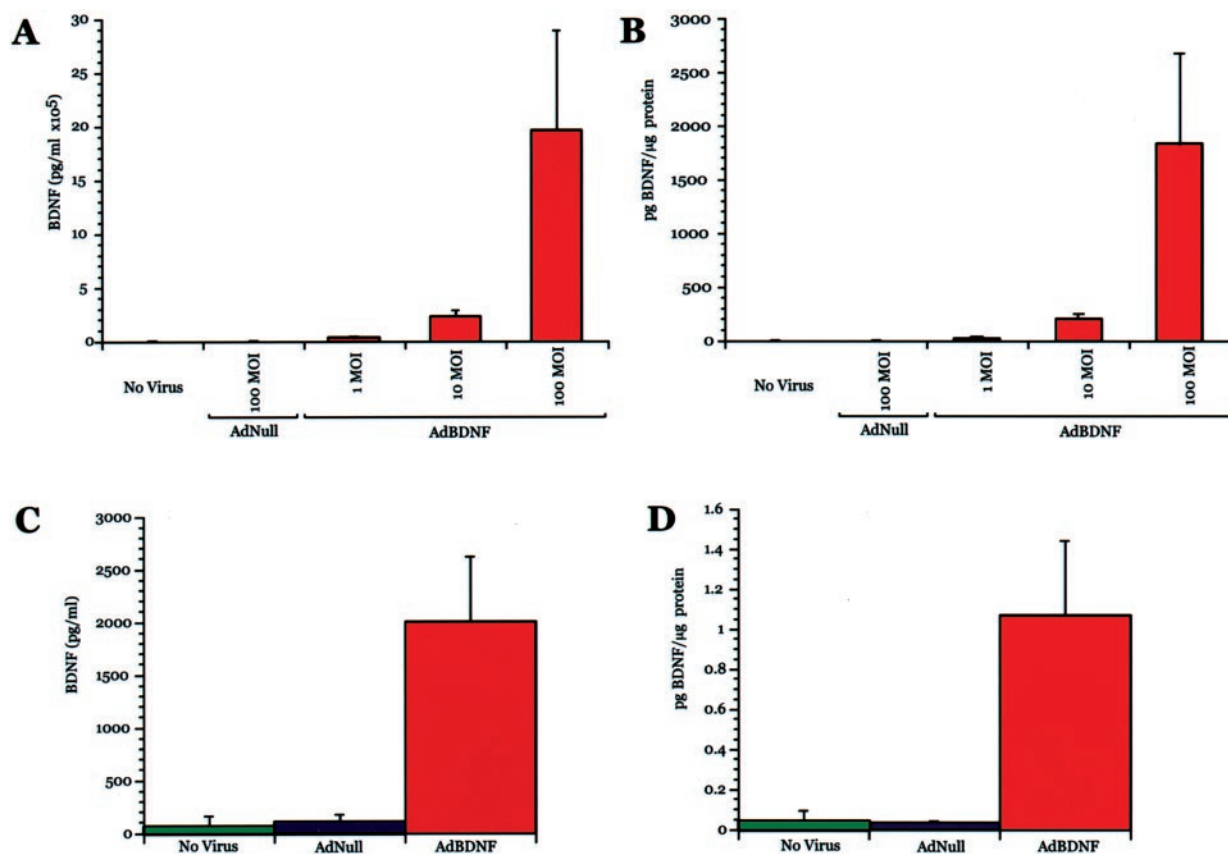
Figure 2. Adenoviral BDNF infection yielded high-level BDNF expression *in vitro* and *in vivo*. *A*, *B*, HeLa cells transduced with AdBDNF secreted BDNF in a viral dose-dependent manner (*n* = 3). *C*, *D*, AdBDNF-injected animals showed sustained expression of high levels of BDNF in CSF, as measured on day 20 (*n* = 5). *A* and *C* show results in picograms per milliliter, and *B* and *D* are given in picograms per microgram of protein.

cells/mm^3 in the AdBDNF-treated rats (Fig. 5). Within the olfactory bulb itself (measured rostrally from the line connecting the dorsal and ventral posterior borders of the olfactory cortex), we found that AdBDNF treatment increased by 2.44 ± 0.1-fold the number of BrdU$^+$ cells relative to the AdNull controls (*p* = 0.0006 by ANOVA; $F_{(1,7)}$ = 42.1). This value reflected the cell counts obtained from scoring entire sagittal sections of the olfactory bulb; the values included both the internal and external granular zones of the scored bulbs. These results indicated that the number of cells migrating to the olfactory bulb was substantially greater in the AdBDNF-treated animals than their AdNull controls.

In both the AdBDNF and AdNull animals, the BrdU$^+$ cells were next double-immunostained for βIII-tubulin and/or MAP-2 to establish the proportion of neurons within the total BrdU$^+$ cell pool (Fig. 6). In both groups, BrdU-incorporating cells found within the olfactory stream almost invariably expressed βIII-tubulin immunoreactivity. The same was true in the olfactory bulb, within which double-labeled cells for MAP-2–BrdU were also frequent. Interestingly, MAP-2-labeled BrdU$^+$ cells were seen only in the bulb and not in the olfactory subependyma or migratory stream. Instead, these cells were first noted within the granular layer of the olfactory bulb itself, consistent with the differentiation of mitotic βIII-tubulin$^+$ neuroblasts to postmitotic MAP-2$^+$ neurons during terminal migration from the olfactory subependyma to the olfactory cortex (Lois et al., 1996; Goldman and Luskin, 1998). Quantitatively, in the AdNull-treated rats, 93.2 ± 0.5% of BrdU$^+$ cells in the olfactory bulb expressed βIII-tubulin. This proportion was virtually identical to that ob-

tained in the AdBDNF-treated olfactory bulbs, in which an average of 93.0 ± 1.8 and 89.4 ± 2.4% of BrdU$^+$ cells coexpressed neuronal βIII-tubulin or MAP-2, respectively. These data indicate that most cells recruited to the olfactory bulbs were neurons and that AdBDNF substantially promoted the addition of these new neurons to the adult olfactory system.

Confocal imaging confirmed that cells added to the olfactory bulbs were neurons

High-magnification confocal imaging confirmed the neuronal antigenicity of the BrdU-labeled cells in both the rostral migratory stream and olfactory bulb. Representative sections were taken from four brains, including two AdBDNF-treated experimentals and two AdNull controls. Midsagittal sections derived from each of these were double-immunostained for BrdU together with either βIII-tubulin or MAP-2 and imaged via confocal laser scanning, with compositing and reconstruction in the *z*-dimension to ensure the neuronal immunoreactivity of BrdU$^+$ cells. This confirmed that those BrdU$^+$ cells added to the olfactory bulb were almost entirely neurons, in that they expressed MAP-2 as well as βIII-tubulin, and did so in both the AdBDNF- and AdNull-treated animals. Merged *z*-stacks of confocal images of MAP-2$^+$ and βIII-tubulin$^+$ neurons, colabeled for BrdU, confirmed that >90% all BrdU$^+$ nuclei in the olfactory bulb were harbored by MAP-2$^+$ or βIII-tubulin$^+$ cells (Fig. 6). This indicated that the AdBDNF-associated increases in the olfactory bulb BrdU labeling indices reflected enhanced neurogenesis and/or recruitment in the treated animals.
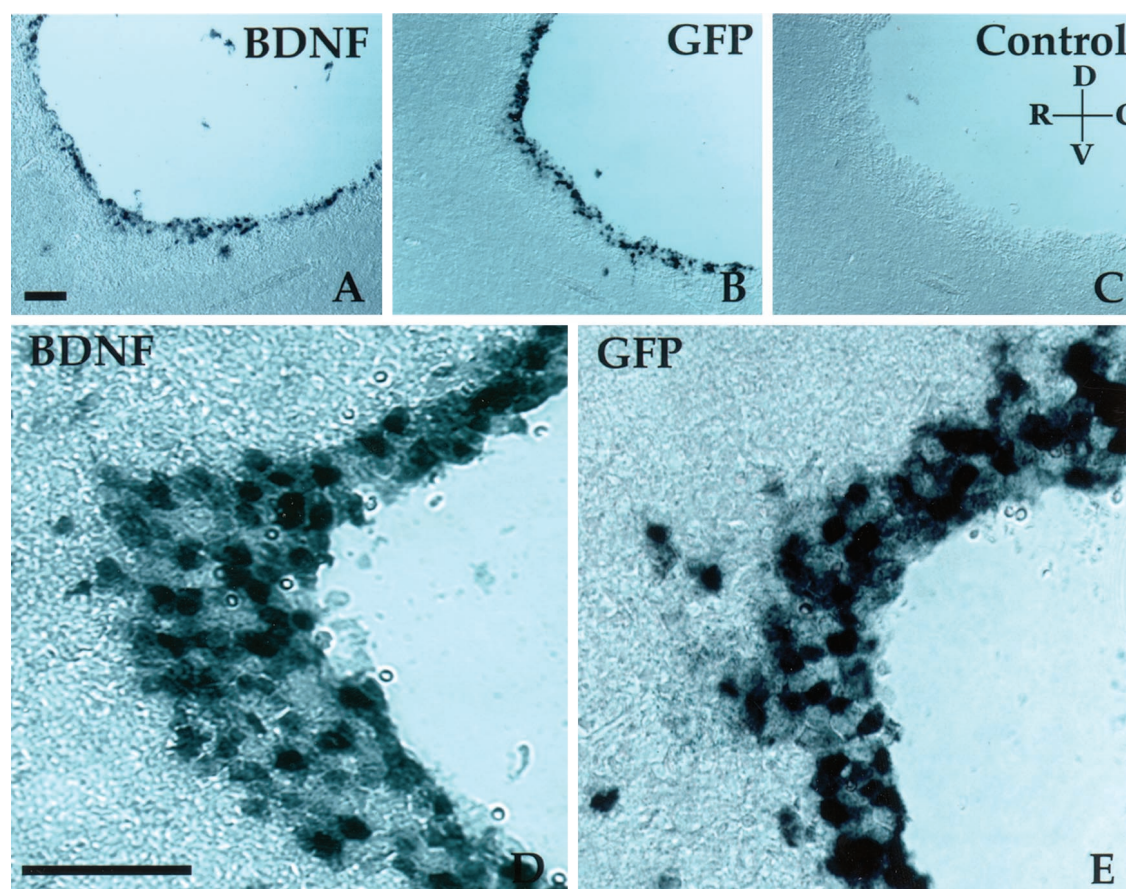
Figure 3. AdBDNF transduced expression of BDNF and hGFP mRNA *in vivo.* Serial sections of AdBDNF–GFP-injected brain were treated with antisense probes for BDNF (*A*, *D*) or GFP (*B*, *E*). mRNA expression was restricted to the wall of the lateral ventricle. *C*, Sense probe for BDNF, as control. *D* , dorsal; *V* , ventral; *R* , rostral; *C* , caudal. Scale bar, 35 μm.

Ventricular AdBDNF infection induced striatal neuronal recruitment

Despite the extraordinary increase in olfactory neuronal recruitment in AdBDNF-treated rats, this treatment was not associated with significantly increased cell division outside of the olfactory system. The mean numbers of BrdU$^+$ cells per section in the frontal cortex, septum, and striatum were all approximately equivalent in the AdBDNF- and AdNull-injected brains when assessed 20 d after viral injection (Fig. 7). Nonetheless, this left open the possibility that AdBDNF might be influencing either the lineage choice of mitotically active progenitors or the selective survival of their neuronal daughters. To assess this possibility, we
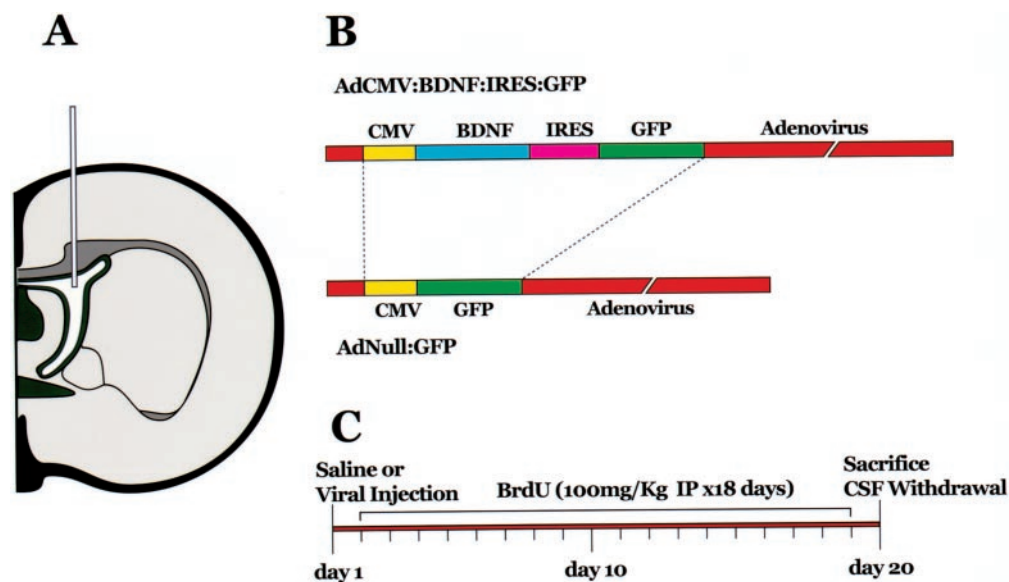

Figure 4. Strategy used to induce adult neuronal recruitment. *A*, Delivery: schematic coronal section showing site of injection of adenovirus into the lateral ventricle. *B*, Vector: E1-deleted (ΔE1) adenoviral type 5 constructs used to express a bicistronic transcript of BDNF and hGFP (or hGFP alone, as a control vector) under the control of the constitutive CMV early promoter. *C*, Experimental protocol: adenovirus was injected on day 1, followed by intraperitoneal injections of 100 mg/kg BrdU for the next 18 d. On day 20, CSF was extracted for BDNF ELISA, and the brains were processed for BrdU immunohistochemistry in tandem with phenotype-specific immunolabeling.
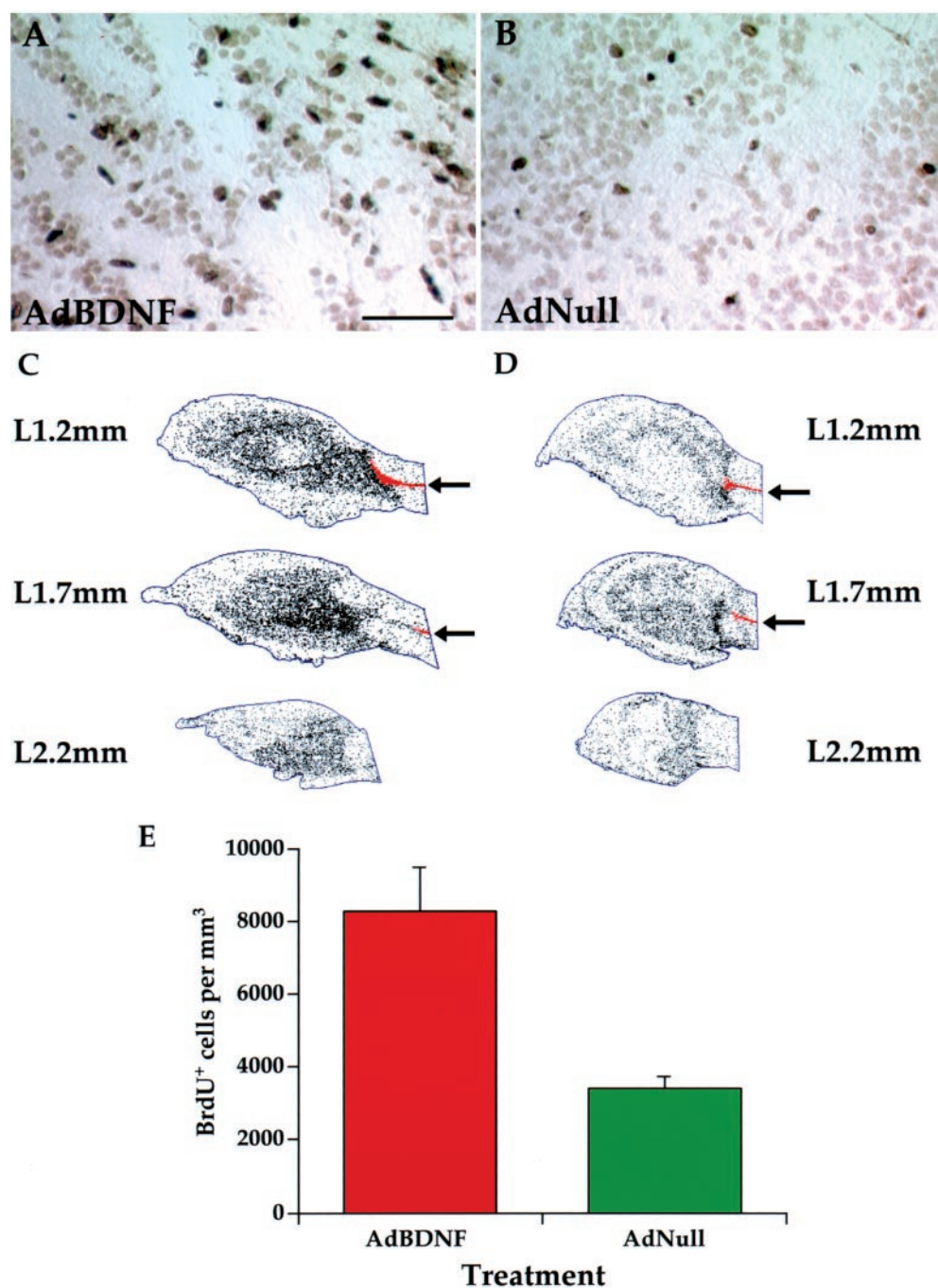
Figure 5. AdBDNF injection increased recruitment to the olfactory bulb. *A, B,* BrdU$^+$ cells in the olfactory bulbs of AdBDNF:IRES:hGFP (*A*) AdNull:GFP (*B*) injected brains, at day 20. *C,* Stereological reconstruction of BrdU$^+$ cells, viewed here at different mediolateral levels of the olfactory bulb, revealed substantially higher BrdU$^+$ cell densities in the olfactory subependyma and granular layers of AdBDNF-treated rats (*C*) than in their AdGFP-injected controls (*D*). *Arrows* denote entry to rostral migratory stream in *red*. *E,* The average number of BrdU$^+$ cells/mm^3 in the olfactory bulb (*n* = 4 per group), plotted as a function of treatment, again revealed significantly higher numbers of newly generated BrdU$^+$ cells in AdBDNF-treated rats than their controls.

scored the incidence of βIII-tubulin$^+$–BrdU$^+$ cells in each non-olfactory region studied, in both AdBDNF- and AdNull-treated brains. When BrdU$^+$ cells were identified by epifluorescence microscopy, they were subjected to two-color confocal imaging with serial sections in the *z* plane, to estimate the incidence of double-labeled βIII-tubulin$^+$–BrdU$^+$ cells and to ensure that the BrdU$^+$ nuclei indeed belonged to βIII-tubulin$^+$ cell profiles.

We found evidence of only very rare BrdU$^+$–βIII-tubulin$^+$ neurons in the frontal cortex of AdBDNF-treated animals, too few to merit systematic comparison with null controls. We found no examples of newly generated septal neurons in either the AdBDNF- or AdNull-injected animals. Surprisingly, however, we found that the AdBDNF-treated animals harbored a distinct population of newly generated neurons in the neostriatum (Figs.

8, 9). These BrdU$^+$ neurons comprised a distinct minority of the BrdU$^+$ striatal cells in these brains; they were scattered throughout the striatum, although they were most often located in its periventricular third. Confocal imaging confirmed examples of newly generated, BrdU$^+$ striatal cells that expressed a variety of independent markers of neuronal phenotype, which included βIII-tubulin, NeuN, GAD67, DARRP-32, and calbindin-D28K (Figs. 9–11).

Quantitatively, unbiased counting of all striatal BrdU$^+$ cells in sagittal sections of AdBDNF-treated animals revealed an average of 1663 $\pm$ 748 BrdU$^+$ cells/mm^3. Among a randomly chosen sample of 477 BrdU$^+$ striatal cells located in sections (*n* = 17) selected from three AdBDNF-treated brains, 41 cells (8.3 $\pm$ 2.3%) could be confirmed as double-labeled for both BrdU and βIII-
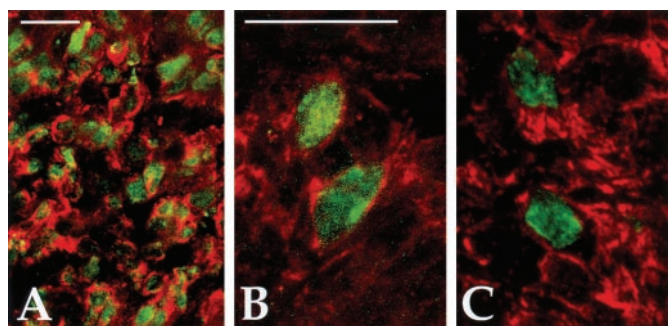
Figure 6. AdBDNF-associated newly generated olfactory cells were neurons. Confocal imaging confirmed that BrdU$^+$ cells added to the olfactory bulb were almost entirely neurons in rats injected with virus 3 weeks before being killed and given BrdU daily until the day before death. *A–C*, Merged *z*-dimension stacks of confocal images of BrdU (*green*) colabeling with βIII-tubulin$^+$ (*A*, *B*; in *red*) and MAP-2$^+$ (*C*; *red*) neurons. This suggested that the AdBDNF-associated increase in the olfactory bulb BrdU labeling index reflected enhanced neurogenesis and/or recruitment to the bulb. Scale bars, 25 μm.
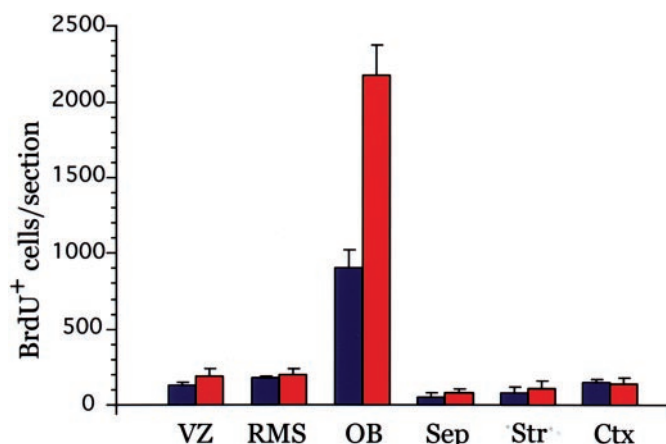

Figure 7. AdBDNF stimulation of BrdU$^+$ cell addition was pronounced in the olfactory bulb but not appreciable elsewhere. AdBDNF treatment promoted net BrdU$^+$ cell addition to the olfactory bulb but not to the septum, striatum, or cortex. The difference between AdBDNF (*red*)- and AdNull (*blue*)-treated olfactory bulb BrdU labeling indices was significant to $p < 0.001$. No other comparisons based on total BrdU$^+$ cell counts were significant. However, whereas BrdU$^+$ cell addition to non-olfactory regions was almost entirely non-neuronal in AdNull control rats, the BrdU$^+$ cell population included newly generated neurons in several regions of the AdBDNF-injected brains. Thus, when BrdU$^+$–βIII-tubulin$^+$ neurons were specifically compared between AdBDNF and AdNull treatment groups, a significant effect of AdBDNF on neuronal recruitment to the striatum was noted (see below). *Red*, AdBDNF treated; *blue*, AdNull treated. *VZ*, Ventricular zone; *RMS*, rostral migratory stream; *OB*, olfactory bulb; *Sep*, septum; *Str*, neostriatum; *Ctx*, neocortex.

tubulin by confocal imaging (Fig. 9) (see Materials and Methods for criteria used). This compared with the complete absence of double-labeled striatal neurons in the PBS-injected rats (0 of 95 cells; $n = 8$ sections taken from 3 rats) and with the relatively rare incidence of BrdU$^+$–βIII-tubulin$^+$ neurons observed in the AdNull-injected rats (15 among 591 randomly chosen BrdU$^+$ striatal cells; $2.1 \pm 1.1\%$; $n = 23$ sections taken from 6 rats) (Fig. 8*B*; discussed below). ANOVA established that the incidence of new striatal neurons in the AdBDNF-injected rats and their controls differed significantly ($p = 0.006$; $F_{(2,9)} = 9.48$). On a per animal basis, $8.3 \pm 2.3\%$ of the BrdU$^+$ cells in the AdBDNF-treated rat striata, or 143 ± 26.5 cells/mm^3, were antigenically definable as
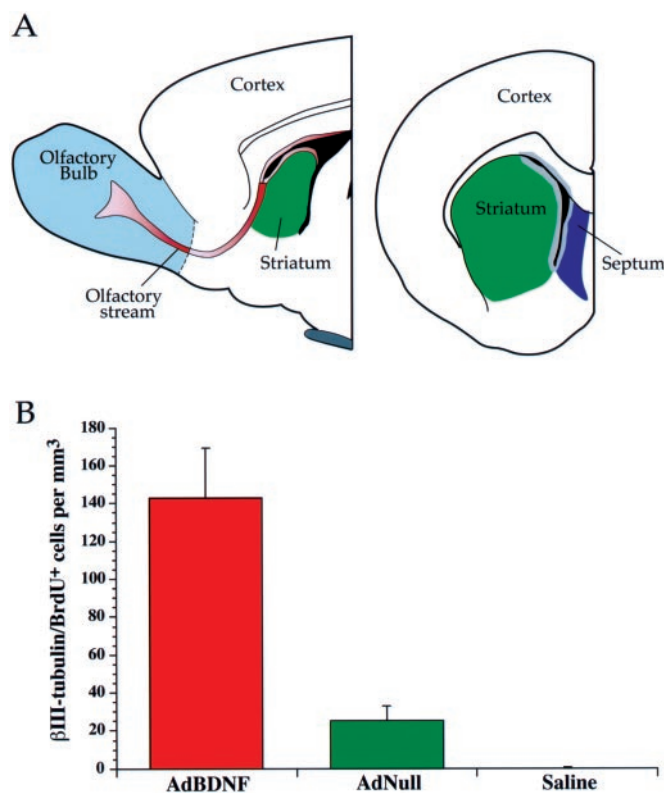

Figure 8. AdBDNF treatment was associated with neuronal addition to the neostriatum. *A* shows sagittal (*left*) and coronal (*right*) schematics of the neostriatal region assessed for neuronal addition (indicated in *green*) in AdBDNF-injected rats and their AdNull-injected controls. *B* plots the mean density of βIII-tubulin$^+$–BrdU$^+$ cells in AdBDNF- and AdNull-injected striata and in PBS-injected controls at day 20 ($n = 4$).

neurons (Fig. 8*B*). This represented only 0.34% (143 of 41,637) of the total striatal neuronal pool. However, because these cells were generated in just 3 weeks, one might predict that proportionately more neurons may be added to the striatum with longer survival times (see below), provided that both viral BDNF expression and progenitor cell competence are sustained.

No neurogenesis was noted in the untreated adult striatum

To assess the incidence, if any, of neuronal addition to the normal untreated neostriatum, we examined control animals that were injected intraventricularly with either PBS ($n = 3$) or AdNull ($n = 5$), who received BrdU on days 2 through 19, and that were then killed on the next day (3 week time point). In the PBS-injected rats, no BrdU$^+$–βIII-tubulin$^+$ striatal neurons were found (Fig. 8). In these same rats, constitutive neurogenesis was observed in both the olfactory bulb and dentate gyrus, as would be expected, although we made no attempt at quantifying baseline neuronal recruitment at these sites. Thus, we found no evidence of constitutive neurogenesis in the normal unstimulated neostriatum, in contrast to the robust neuronal recruitment observed in the AdBDNF-treated striatum.

Adenoviral infection per se was associated with a minor induction of neuronal recruitment

Interestingly, and in contrast to the absence of striatal neuronal addition noted in the PBS-treated rats, the AdNull-injected controls did exhibit a small amount of constitutive neuronal addition to the striatum. As noted above, among 591 BrdU$^+$ striatal cells
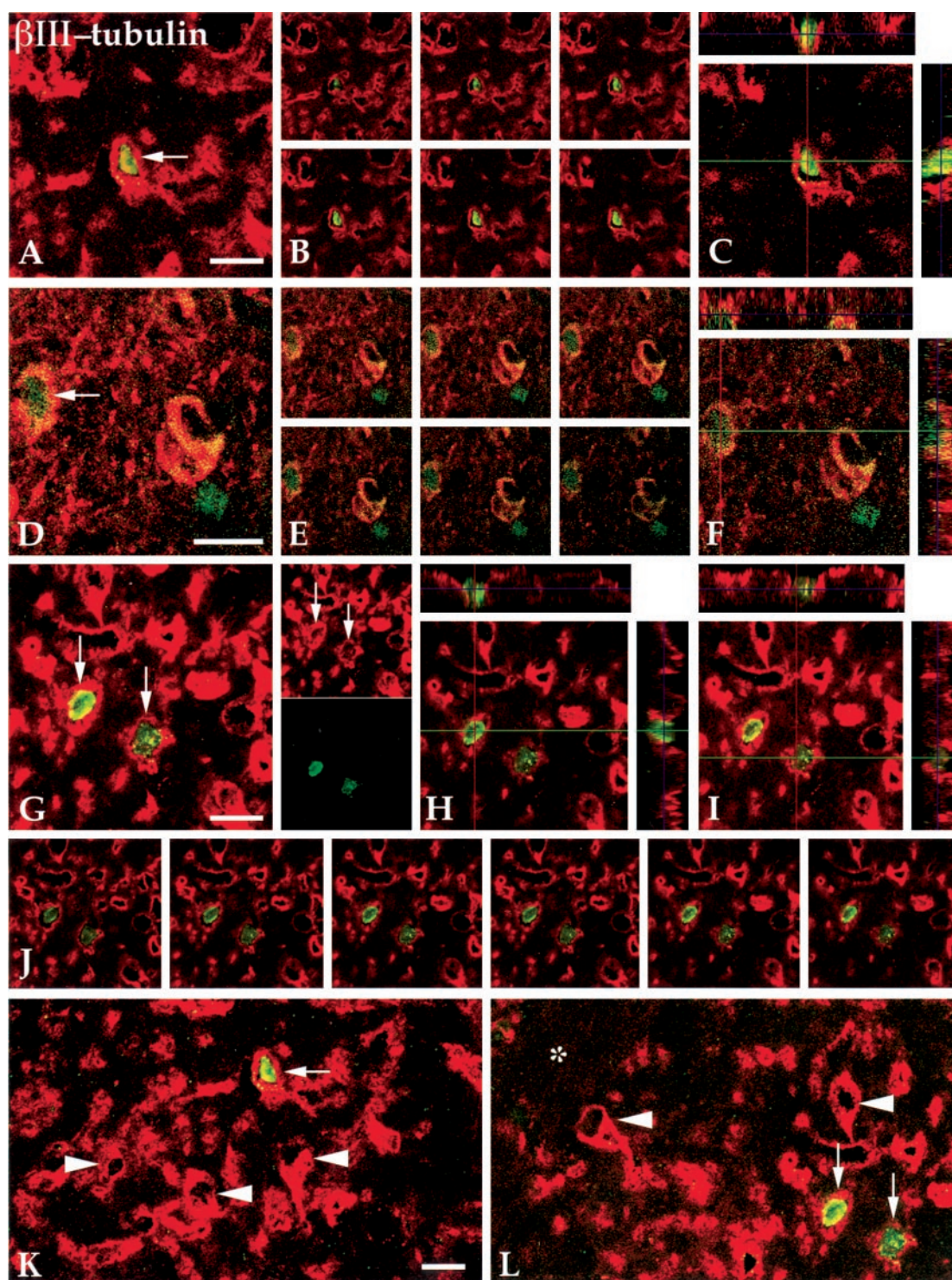
Figure 9. AdBDNF induced the heterotopic addition of BrdU$^+$–βIII-tubulin$^+$ neurons to the striatum. Confocal images of BrdU-labeled neurons found in the neostriata of AdBDNF-treated rats 3 weeks after virus injection. These cells were identified by immunostaining for both BrdU (*green*) and βIII-tubulin (*red*). *A–C,* A representative βIII-tubulin$^+$–BrdU$^+$ cell (*arrow*). *A* shows a *z*-dimension composite of serial 0.9 μm images, showing βIII-tubulin$^+$ (*red*) and BrdU (*green*) immunoreactivities. *B,* A *z*-dimension series of six separate 0.9 μm confocal images taken 0.6 μm apart, displaying the concurrence of BrdU and βIII-tubulin in the new neuron. *C,* A single optical section with reconstructed orthogonal images, as viewed from the sides in both the *x–z* and *y–z* planes. *D–F,* Another newly generated, βIII-tubulin$^+$–BrdU$^+$ neostriatal neuron (*arrow*), similarly viewed as a *z*-stack composite (*D*). By way of contrast, this field also includes both a non-neuronal BrdU$^+$ cell and a βIII-tubulin$^+$ but BrdU-unlabeled resident neuron. Like *A–C,* this field is also viewed as a series of optical sections (*E*) and in orthogonal side views (*F*). *G–J,* A pair of βIII-tubulin$^+$–BrdU$^+$ striatal neurons (*arrows*), composited in *G* with split *red* and *green* images separately indicating βIII-tubulin$^+$ and BrdU, respectively. *H, I,* An optical section with orthogonal images taken at two different points to allow individual assessment of the βIII-tubulin staining of each of these BrdU$^+$ cells. Both BrdU$^+$ nuclei are completely surrounded by βIII-tubulin. *J,* A series of *z*-dimension optical sections through these cells, again confirming the coincident expression of BrdU and βIII-tubulin. *K, L,* Low-power views of the fields shown in *A–C* and *G–J,* respectively, to visualize the range of morphologies of both resident (examples as *arrowheads*) and newly added (*arrows*) neurons. * in *L* shows a myelinated bundle passing through the striatal matrix. Scale bars, 10 μm.
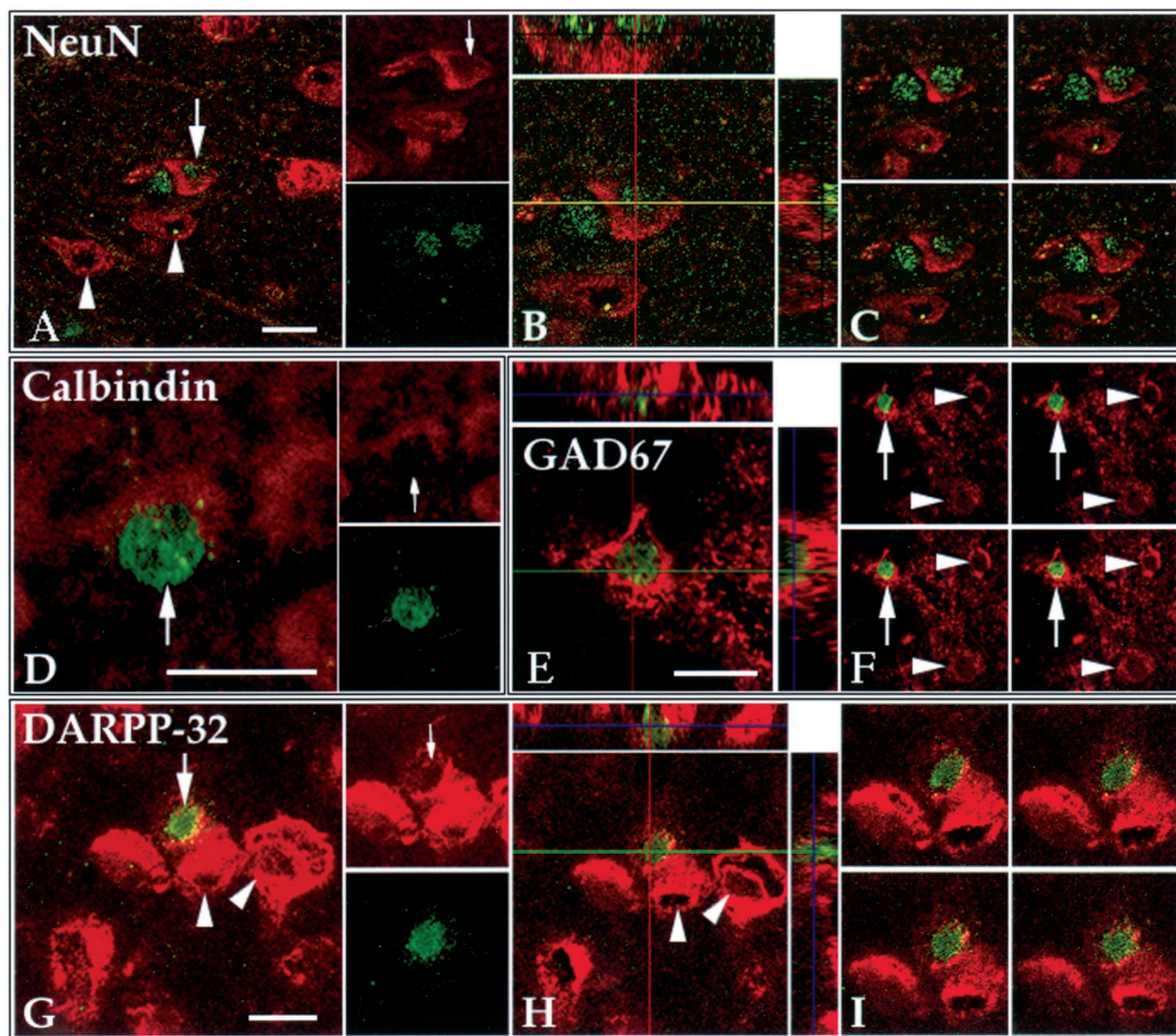
Figure 10. Newly recruited striatal neurons included medium spiny neurons. The BrdU$^+$ neurons found in AdBDNF-treated striata expressed neuronal markers other than βIII-tubulin, which included NeuN. They also expressed characteristic antigenic markers of medium spiny neurons of the adult caudate putamen, including calbindin-D28k, GAD67, and DARPP-32. *A–C*, A typical NeuN$^+$–BrdU$^+$ striatal neuron (*arrow*); local resident neurons (NeuN$^+$–BrdU$^-$) shown by *arrowheads*. *A* shows a z-dimension composite of serial 1 μm images, with split *red* (NeuN) and *green* (BrdU) images on the *right*. *B* shows a single optical section with reconstructed orthogonal images, as viewed from the sides in both the *x–z* (*top*) and *y–z* (*right*) planes. *C* shows a z-dimension series, viewed as four separate 0.9 μm optical sections taken 0.6 μm apart. *D*, A BrdU$^+$ (*green*)–calbindin$^+$ (*red*) neuron, with the split *red* and *green* images of each to show calbindin (*arrow*) and BrdU staining separately. *E* and *F* show confocal images of a GAD67$^+$ (*red*)–BrdU$^+$ (*green*) neuron in an AdBDNF-treated striatum. *E* shows a confocal section with reconstructed orthogonal side views. In the orthogonal side views, the *green* BrdU$^+$ nuclei remain completely surrounded by the *red* GAD67 antigen. *F* shows a z-dimension series of four separate 0.9 μm confocal images taken 0.6 μm apart, displayed to reveal the correspondence of BrdU and GAD67 in the same cell (*arrow*; *arrowheads* indicate resident GAD67$^+$ cells) at multiple z-levels. *G–I* show analogous images of a DARPP-32 (*red*)–BrdU$^+$ (*green*) neuron in the same striatum (*arrowheads*, show examples of BrdU-unlabeled resident neurons). *G* shows the z-dimension composite of serial 0.9 μm images, again with split *red* and *green* images to show DARPP-32 (*arrow*) and BrdU staining individually. *H* shows an optical section with reconstructed orthogonal side views, as described. In both the *x–z* and *y–z* planes, the BrdU$^+$ nucleus is completely surrounded by DARPP-32 signal. *I* shows a z-dimension series through this cell. All images were taken of striatal sections sampled from AdBDNF-treated rats killed 3 weeks after virus administration. Scale bars, 10 μm.

identified in AdNull-injected rats killed at 3 weeks, confocal analysis revealed that 15 cells (2.1 ± 1.1%) double-labeled for BrdU and βIII-tubulin. This was determined using the same criteria as in our concurrent analysis of AdBDNF-treated striata, and the cells were assessed by the same individuals who were blinded as to treatment group. As noted above, this incidence of striatal neuronal addition in the AdNull-treated rats was significantly less ($p = 0.006$) than the 8.3 ± 2.2% noted in their AdBDNF-treated counterparts (Fig. 8). Nonetheless, the very presence of BrdU$^+$–βIII-tubulin$^+$ neurons in the AdNull-treated
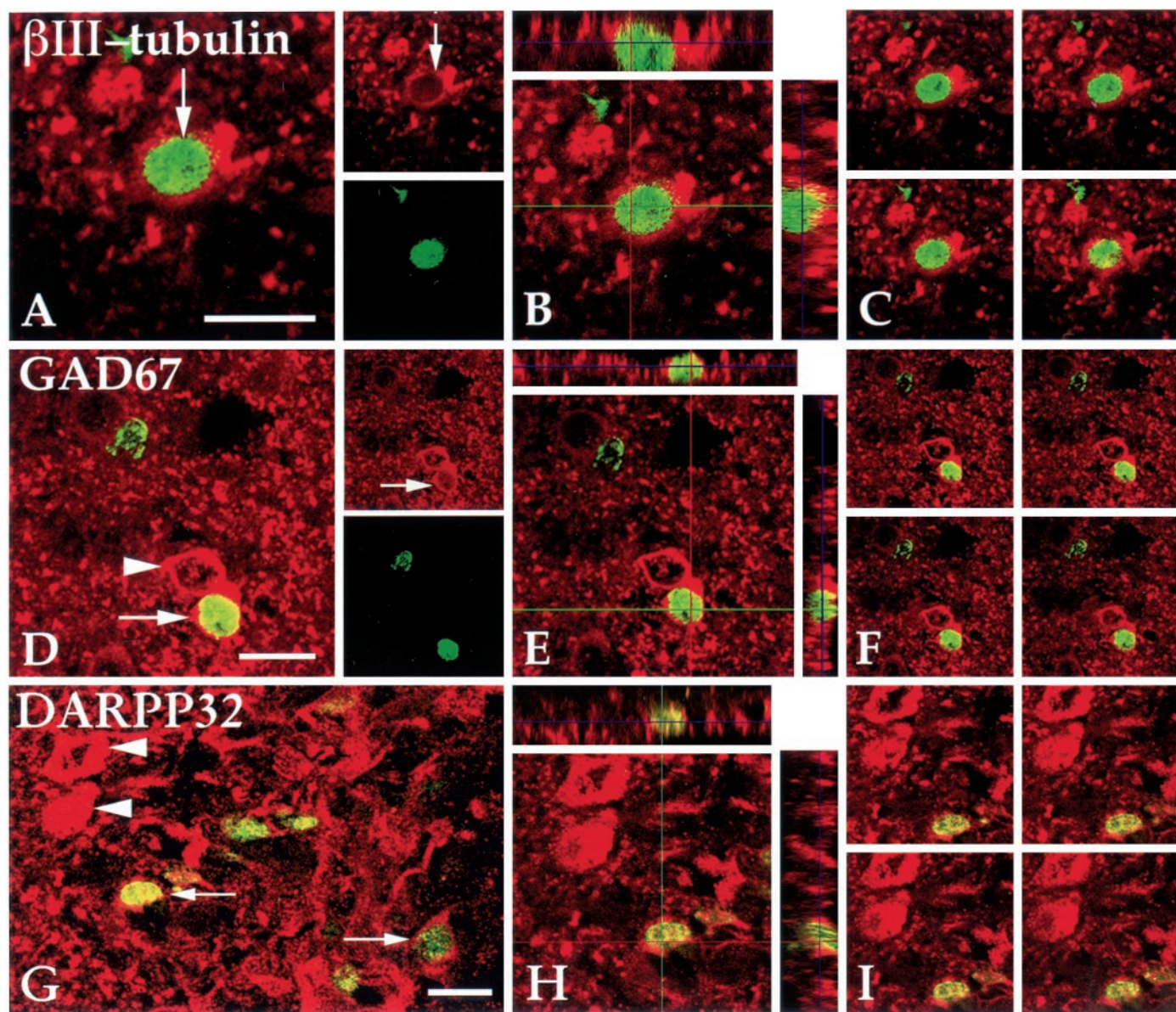
Figure 11. AdBDNF-induced striatal neurons matured and survived for at least 5–8 weeks. βIII-tubulin$^+$–BrdU$^+$, GAD67$^+$–BrdU$^+$, and DARPP32$^+$–BrdU$^+$ striatal neurons persisted in AdBDNF-injected rats. *A–C*, A typical βIII-tubulin$^+$–BrdU$^+$ neuron found in an AdBDNF-treated striatum 8 weeks after virus injection. *A*, The *z*-dimension composite of serial 1 μm images, with split *red* and *green* images to show βIII-tubulin$^+$ (*arrow*) and BrdU, respectively. *B*, A confocal section with reconstructed orthogonal images, as viewed from the sides in both *x–z* (*top*) and *y–z* (*right*) planes. *C*, A *z*-dimension series of four separate 0.9 μm confocal images taken 0.6 μm apart, confirming the βIII-tubulin immunoreactivity of the BrdU$^+$ cell. *D–F*, Analogous images of a GAD67$^+$–BrdU$^+$ neuron viewed in an AdBDNF-treated striatum at 8 weeks. Only one of the two adjacent GAD67$^+$ neurons (*arrow*) is BrdU-labeled; its neighbor is unlabeled (*arrowhead*). *G–I*, A representative DARPP-32$^+$–BrdU$^+$ neuron, again found in an AdBDNF-treated striatum 8 weeks after virus injection. *G*, A *z*-dimension composite of serial optical sections, showing DARPP-32 (*red*) and BrdU (*green*) immunoreactivities. DARPP-32$^+$–BrdU$^+$ neurons are indicated by *arrows*; BrdU-unlabeled resident neurons are indicated by *arrowheads*. *H*, Orthogonal views of the DARPP-32$^+$–BrdU$^+$ striatal neuron. *I*, Serial 0.9 μm optical sections taken 0.6 μm apart confirm the coincidence of BrdU and DARPP-32 in the same cell. Scale bars, 10 μm.

striata was surprising, given the absence of any new striatal neurons in the PBS-injected rats, and suggested that adenoviral infection itself might have resulted in some mobilization of neural progenitors. This raised the possibility that virally induced ependymal cytokines may influence subependymal neuronal production or migration; this in turn might allow otherwise heterotopic neuronal recruitment. Nonetheless, the substantial increase in striatal neuronal addition in the AdBDNF-treated rats relative to their AdNull-treated controls argued that any adenovirus-associated mobilization of neural progenitor cells was minor

relative to that specifically attributable to BDNF. Together, these observations indicated that AdBDNF induced the addition of new neurons to the neostriatum, an otherwise atypical site for neuronal recruitment in the adult brain.

AdBDNF-induced striatal neurons expressed antigens of medium spiny neurons

To assess the neuronal phenotype induced by AdBDNF infection, we immunostained sections of AdBDNF-treated brains for a number of markers of striatal phenotype. We found that some

BrdU$^+$ striatal cells expressed calbindin-D28K, a marker of medium spiny neurons of the caudate putamen (Waldvogel et al., 1991; Burke and Baimbridge, 1993) (Fig. 10). Similarly, we found an abundance of BrdU$^+$ striatal cells that coexpressed GAD67, a characteristic marker for GABAergic neurons (Fig. 10).

Despite their expression by medium spiny neurons, both calbindin and GAD67 are expressed by other cell types and even within the striatum may not be definitive markers of medium spiny neurons. Thus, to better ascertain the phenotype of AdBDNF-induced striatal neurons, we double-stained sections derived from the same animals for DARPP-32, a highly selective marker of medium spiny neurons (Ivkovic and Ehrlich, 1999). Among the rats killed 3 weeks after virus injection, six of a random sample of 125 BrdU$^+$ striatal cells (4.8%) were found to be DARPP-32$^+$ and were confirmed as such by confocal imaging and serial reconstruction (Fig. 10). [This compared with 41 of 477 BrdU$^+$ cells (8.3%) in adjacent sections of the same rats that expressed βIII-tubulin.] Importantly, the percentage of DARPP-32$^+$ cells among the BrdU$^+$ striatal cell population increased with time, such that when assessed in rats killed 8 weeks after AdBDNF injection, 10 of 128 BrdU$^+$ cells (7.8%) were DARPP-32$^+$ (see below). Together, these observations suggested that many, if not most, of the AdBDNF-induced striatal cells matured to a phenotype characteristic of medium spiny neurons. These data raise the possibility that AdBDNF treatment might contribute to the restoration of this phenotype, a critical mediator of striatopallidal communication, whose significance is underscored by its selective loss in Huntington's Disease.

AdBDNF-induced striatal neurons matured and survived

The 3 week time point used to establish neuronal recruitment in response to AdBDNF allowed the possibility that those cells generated and detected at 3 weeks were merely transitional phenotypes, perhaps transient in their very existence. To establish the more prolonged survival of AdBDNF-associated striatal neurons, we thus set up a distinct group of animals that were killed and assessed 8 weeks after viral injection. Both βIII-tubulin$^+$–BrdU$^+$ and DARPP32$^+$–BrdU$^+$ double-labeled striatal cells persisted in these rats, with little apparent loss (Fig. 11). Among a sample of 106 BrdU$^+$ cells in three 8 week rat striata randomly sampled for confocal imaging, seven cells (6.6%) were found to express βIII-tubulin. Similarly, 10 of 128 sampled BrdU$^+$ cells (7.8%) expressed DARPP-32. The rough equivalency of the proportion of BrdU$^+$ striatal cells that were βIII-tubulin$^+$ and DARPP$^+$ argued that, by 8 weeks after AdBDNF injection or 5 weeks after the last BrdU incorporation, virtually all of the BrdU$^+$ neurons, as defined by βIII-tubulin, also would have been expected to express DARPP-32. Thus, a substantial number of AdBDNF-induced striatal neurons survived, depending on the time point of their generation during the BrdU injection course, for at least 5–8 weeks after terminal mitosis. Furthermore, these surviving neurons matured sufficiently to express DARPP-32, a relatively mature marker of striatal neuronal phenotype. As such, these AdBDNF-induced neurons did not appear to constitute transitional phenotypes.

AdBDNF treatment was associated with systemic weight loss

The AdBDNF-injected animals were noted to experience a stereotypic weight loss during the 3 week period between AdBDNF delivery and death. This was not unexpected, because weight loss has been described previously in rats receiving intraventricular BDNF infusions. This syndrome appears to be central in origin and reflects BDNF-associated appetite suppression and hypophagia rather than any hypermetabolic state (Pelleymounter et al., 1995). We found that this was not an effect of the virus in that neither AdNull- nor PBS-injected animals experienced similar weight loss. Whereas AdNull-injected controls rose from 300 ± 16 gm at the time of viral injection to 339 ± 6 gm at the time of being killed 3 weeks later ($n = 4$), a matched set of AdBDNF-treated animals lost weight during that period, falling from 328 ± 34 to 288 ± 17 gm per animal ($p = 0.016$ by ANOVA, comparing the slopes of weight gain as a function of time between AdBDNF-, AdNull-, and PBS-treated rats; $F_{(2,13)} = 6.17$)

The time course of weight loss in the AdBDNF-treated animals suggested to us that virally delivered BDNF was exerting rapid and powerful biological effects on the target nervous system, within the same time frame as the BDNF-associated rise in neuronal recruitment. Whether this anorexic phenotype was a consequence of olfactory neuronal addition and altered olfactory perception or was instead an unrelated effect of central BDNF overexpression remains to be established.

DISCUSSION

We report here that infection of the adult rat ventricular lining with an adenoviral BDNF expression vector induced the recruitment of new neurons from resident progenitor cells of the forebrain ventricular zone. In particular, adenoviral infection resulted in the diffuse transduction of the adult ventricular wall, with the effective subrogation of the ependyma into a source of secreted BDNF to both the CSF and periventricular parenchyma. This resulted in the sustained, high-level secretion of BDNF by the ventricular wall and was associated with a >2.4-fold increase in the recruitment of new neurons to the rat olfactory bulb over the 3 weeks after viral administration. Importantly, AdBDNF administration was also associated with the heterotopic addition of new neurons to the neostriatum, with the recruitment of BrdU-incorporating βIII-tubulin$^+$–DARPP-32$^+$–NeuN$^+$–GAD67$^+$–calbindin-D28K$^+$ neurons to the striata of the AdBDNF-treated animals. To the best of our knowledge, these experiments comprise the first use of viral gene delivery as a means to induce neurogenesis from resident progenitor cells in the adult CNS. In addition, they present the first evidence for induced neuronal addition to the mature neostriatum. Together, these results indicate that viral transduction of the adult ependyma to overexpress BDNF may be an effective means of inducing the recruitment of new neurons to permissive regions of the mature brain.

We observed predominantly ependymal cell expression of both BDNF and GFP mRNAs after intraventricular injection of AdBDNF:IRES:GFP. Nonetheless, occasional subependymal labeling was noted, particularly along the subcallosal and dorsolateral walls of the lateral ventricles. When present, subependymal GFP fluorescence appeared as rapidly as ependymal cell labeling; both were evident by 7 d after virus injection (Fig. 1). GFP$^+$ cells were limited to the ventricular layers, however, and were never noted in either the olfactory subependyma or striatal parenchyma, except for migrants into the corpus callosum. Despite this restriction of virally expressed BDNF to the ventricular wall, newly generated neurons, derived from uninfected subependymal cells, were profoundly influenced by their genesis adjacent to AdBDNF-infected ependymal cells. Thus, the effects of ependymal BDNF on neurogenesis and neuronal recruitment to the olfactory bulb and striatum likely derived from a paracrine effect of BDNF on uninfected subependymal progenitors.

The effects of BDNF were presumably exerted early in the ontogeny of newly generated neurons, before their departure from the ventricular wall, because it is unlikely that ependymal secretion of BDNF to the CSF and periventricular parenchyma would have influenced BDNF levels in the olfactory bulb or striatal parendyma. Indeed, the mature olfactory bulb harbors high levels of BDNF, whereas the neurotrophin appears relatively sequestered from the adult ventricular zone and olfactory subependyma. Thus, a likely scenario is that ependymal BDNF acts to promote the early differentiation and survival during migration of newly generated, subependymally derived neurons, and that these cells survive to migrate into an already BDNF-rich environment in the olfactory bulb. As such, neuronal mitogenesis and departure from the ventricular wall may be viewed as the initial rate-limiting steps for neuronal recruitment, with the cells finding a permissive environment for survival once in the bulb.

Importantly, AdBDNF injection was also associated with the addition of new neurons to the neostriata of treated animals. Such neuronal addition to non-granule cell populations has only rarely been reported in the adult mammalian brain, specifically in the visual cortex (Kaplan, 1981) and macaque frontal cortex (Gould et al., 1999), as well as in response to injury in the adult mouse frontal cortex (Magavi et al., 2000). More generally, however, reports of neurogenesis in the adult mammalian brain have been limited to olfactory, hippocampal, and cerebellar granule cell populations (for review, see Goldman and Luskin, 1998). Nonetheless, careful analysis of serially reconstructed confocal images revealed that our AdBDNF-injected animals harbored a discrete cohort of antigenically confirmed neurons, which colabeled with BrdU and were scattered throughout the neostriatum. Because the adult neostriatum typically does not add new neurons, the induced neuronal addition associated with AdBDNF treatment may be viewed as heterotopic in nature.

Although their numbers were small relative to the much larger pool of AdBDNF-induced olfactory neurons, the recruitment kinetics of the induced striatal pool were surprisingly robust. Given an average striatal neuronal BrdU labeling index of 0.34% and an average of $1.03 \times 10^6 \pm 6.56 \times 10^4$ neurons per striatum, ~3.5×10^3 neurons may be added to each striatum over an 18 d period of BrdU injection, or ~195 neurons per striatum per day. This estimate is crude and likely an underestimate in that it is predicated on the assumptions that daily BrdU injections label the entire mitotic pool and that no striatal cells die during this period. In addition, these numbers reflect but one point on the dose–response curve relating neuronal recruitment to BDNF expression levels; it is important to remember that in this study we have not perturbed either the dose of adenovirus or that of its expressed BDNF. Nonetheless, these numbers suggest that AdBDNF-induced neuronal addition may be sufficiently robust to contribute meaningfully to striatal function, if not architecture. Furthermore, the identification of many AdBDNF-induced neurons as DARPP-32$^+$–GAD67$^+$–calbindin-D28K$^+$ suggests that at least a significant fraction of these neurons may be homologous to the medium spiny neuron population of the adult neostriatum. Because this is the neuronal population lost in Huntington's disease and the striatonigral degenerations, transduction of the ventricular wall with BDNF expression vectors might be envisaged as a feasible strategy for restoring diminished neuronal populations in the striatal degenerations, as well as in other conditions of acquired striatal neuronal loss.

Interestingly, we noted that the AdNull-injected controls exhibited a small amount of constitutive neuronal addition to the stria-

tum. This did not appear to reflect neurogenesis in the normal striatum, because PBS-injected rats exhibited no striatal neuronal addition whatsoever. Rather, these results suggested that adenoviral infection per se might have been sufficient to instigate mobilization of neural progenitors. Although minor in extent and significantly less robust than AdBDNF-induced neuronal recruitment, the AdNull induction of striatal neuronal addition may represent a hitherto unrecognized feature of central viral infection, especially of the ependyma–subependyma. Presumably, virally induced ependymal cytokines might stimulate subependymal neurogenesis and thereby permit otherwise heterotopic neuronal recruitment. This possibility is strengthened by reports that adenovirally induced cytokines include interleukin-6 (IL-6) and IL-8, both of which have been found to be neurotrophic *in vitro* (Driesse et al., 2000). Indeed, such paracrine activation of neurotrophic cytokines might explain recent observations of both inflammation and apoptosis-related neuronal recruitment in the adult brain (Wang et al., 1998; Magavi et al., 2000). In any event, the significant increase in neuronal recruitment to the striatum in the AdBDNF-treated rats, relative to their AdNull-treated controls, argued that any virus-associated cell genesis paled beside that specifically associated with BDNF.

It is worth noting that, despite the frequent observation of BrdU-incorporating cells in the septa, striata, and frontal cortices of these animals, no significant differences were noted between the AdBDNF and AdNull control animals in their BrdU-labeled cell numbers (Fig. 7). To be sure, AdBDNF treatment was associated with an increase in the relative proportion of neurons among the BrdU$^+$ cells of the neostriatum (Figs. 8, 9). Nonetheless, the percentage of confocal-validated new neurons in the overall striatal BrdU$^+$ cell population was so small (just 8% of the BrdU$^+$ population) that AdBDNF would not have been expected to yield readily demonstrable treatment-related differences in either the total BrdU$^+$ cell number or overall striatal neuronal number. The induction of striatal neurogenesis by AdBDNF might therefore reflect either the neuronal differentiation of postmitotic daughters that might otherwise have become glia or the postmitotic rescue of daughters otherwise destined to die. Indeed, although a number of studies have failed to observe any mitogenic effect of BDNF on ventricular zone progenitor cells (Ahmed et al., 1995; Kirschenbaum and Goldman, 1995), these data do not allow us to rule out a direct mitogenic effect *in vivo*.

It is important to also consider the possibility that BDNF might act not only to recruit a ventricular zone-derived population but also to activate resident parenchymal glial progenitors to differentiate as neurons. Studies of both adult rat (Palmer et al., 1999) and human (Roy et al., 1999) brain have indicated the ability of white matter progenitor cells to differentiate as neurons *in vitro*. In the AdBDNF-treated neostriata in particular, the possibility of AdBDNF-induced neurogenesis from parenchymal progenitors is suggested by the frequent observation of clustered pairs of BrdU$^+$ neurons (Fig. 9*G*), although continued division of ventricular zone migrants might also explain this observation (Menezes et al., 1995). Thus, although the possibility that AdBDNF might stimulate neuronal recruitment from parenchymal as well as ventricular zone progenitors is intriguing, our data do not yet allow us to address the source or migration routes of AdBDNF-induced striatal neurons.

The implications of AdBDNF-induced striatal neurogenesis may be profound, particularly for disorders such as Huntington's disease and striatonigral degeneration, in which the loss of striatal neurons may dictate the pathology. The apparent assumption of a medium spiny neuronal phenotype by many, and perhaps most,

AdBDNF-induced neostriatal neurons is especially intriguing, in that it suggests the potential therapeutic utility of this neuronal population. Axiomatically, our hope is that if these cells prove functional and able to survive, then AdBDNF-induced striatal neurons might be able to delay, abrogate, or reverse striatal neurodegenerative disease. Nonetheless, it remains to be seen whether these AdBDNF-induced neurons can functionally integrate, both with resident striatal neurons and nigrostriatal afferents, whether they can survive longer than the 5–8 weeks that we have noted, and whether they can survive the primary disease process better than the cells they are intended to replace. These uncertainties notwithstanding, the adenoviral BDNF-mediated induction of neuronal addition to the adult brain expands our conception of cellular plasticity in the adult CNS and lends a new perspective to the potential for gene therapy in the treatment of structural neurological disease.

REFERENCES

Ahmed S, Reynolds BA, Weiss S (1995) BDNF enhances the differentiation but not the survival of CNS stem cell-derived neuronal precursors. J Neurosci 15:5765–5778.

Alvarez-Buylla A, Lois C (1995) Neuronal stem cells in the brain of adult vertebrates. Stem Cells 13:263–272.

Bajocchi G, Feldman S, Crystal R, Mastrangeli A (1993) Direct in vivo gene transfer to ependymal cells in the central nervous system using recombinant adenovirus vectors. Nat Genet 3:229–234.

Bernhardt R, Matus A (1984) Light and electron microscopic studies of the distribution of microtubule-associated protein 2 in rat brain: a difference between dendritic and axonal cytoskeletons. J Comp Neurol 226:203–221.

Burke R, Baimbridge K (1993) Relative loss of the striatal striosome compartment, defined by calbindin-D28 immunostaining, following developmental hypoxic-ischemic injury. Neuroscience 56:305–315.

Craig CG, Tropepe V, Morshead CM, Reynolds BA, Weiss S, van der Kooy D (1996) In vivo growth factor expansion of endogenous subependymal neural precursor cell populations in the adult mouse brain. J Neurosci 16:2649–2658.

Driesse M, Esandi M, Kros J, Avezaat C, Vecht C, Zurcher C, van der Velde I, Valerio D, Bout A, Sillevis Smitt PA (2000) Intra-CSF administered recombinant adenovirus causes an immune response-mediated toxicity. Gene Therapy 7:1401–1409.

Eriksson P, Perfilieva E, Bjork-Eriksson Alborn A, Nordberg C, Peterson D, Gage F (1998) Neurogenesis in the adult human hippocampus. Nat Med 4:1313–1317.

Goldman SA, Luskin MB (1998) Strategies utilized by migrating neurons of the postnatal vertebrate forebrain. Trends Neurosci 21:107–114.

Goldman SA, Nottebohm F (1983) Neuronal production, migration and differentiation in a vocal control nucleus of the adult female canary brain. Proc Natl Acad Sci USA 80:2390–2394.

Goldman SA, Zaremba A, Niedzwiecki D (1992) In vitro neurogenesis by neuronal precursor cells derived from the adult songbird brain. J Neurosci 12:2532–2541.

Goldman SA, Kirschenbaum B, Harrison-Restelli C, Thaler H (1997a) Neuronal precursor cells of the adult rat ventricular zone persist into senescence, with no change in spatial extent or BDNF response. J Neurobiol 32:554–566.

Goldman SA, Nedergaard M, Harrison-Restelli C, Jiang W, Keyoung HM, Leventhal C, Pincus D, Shahar A, Wang S (1997b) Neural precursors and neuronal production in the adult mammalian forebrain. Ann NY Acad Sci 835:30–55.

Gould E, Reeves A, Graziano M, Gross C (1999) Neurogenesis in the neocortex of adult primates. Science 286:548–552.

Graham F, Prevec L (1991) Manipulation of adenovirus vectors. In: Methods in molecular biology (Murray E, ed), pp 109–128. Totowa, NJ: Humana.

Guan J, Bennet L, George S, Waldvogel H, Faull R, Gluckman P, Keunen H, Gunn A (1999) Selective neuroprotective effects with IGF-1 in phenotypic striatal neurons following ischemic brain injury in fetal sheep. Neuroscience 95:831–839.

Ivkovic S, Ehrlich M (1999) Expression of the striatal DARPP-32/ARPP-21 phenotype in GABAergic neurons requires neurotrophins in vivo and in vitro. J Neurosci 19:5409–5419.

Kaplan M (1981) Neurogenesis in the 3 month-old rat visual cortex. J Comp Neurol 195:323–338.

Kirschenbaum B, Goldman SA (1995) Brain-derived neurotrophic factor promotes the survival of neurons arising from the adult rat forebrain subependymal zone. Proc Natl Acad Sci USA 92:210–214.

Kuhn HG, Winkler J, Kempermann G, Thal L, Gage F (1997) Epidermal growth factor and fibroblast growth factor-2 have different effects on neural progenitors in the adult rat brain. J Neurosci 17:5820–5829.

Lee M, Rebhun L, Frankfurter A (1990) Posttranslational modification of class III β-tubulin. Proc Natl Acad Sci USA 87:7195–7199.

Leventhal C, Rafii S, Rafii D, Shahar A, Goldman SA (1999) Endothelial trophic support of neuronal production and recruitment by the adult mammalian subependyma. Mol Cell Neurosci 13:450–464.

Levy J, Muldoon R, Zolotukhin S, Link C (1996) Retroviral transfer and expression of a humanized, red-shifted green flourescent protein gene into human tumor cells. Nat Biotechnol 14:610–614.

Lindsay RM, Wiegand SJ, Altar CA, DiStefano PS (1994) Neurotrophic factors: from molecule to man. Trends Neurosci 17:182–190.

Lois C, Garcia-Verdugo JM, Alvarez-Buylla A (1996) Chain migration of neuronal precursors. Science 271:978–981.

Magavi S, Leavitt B, Macklis J (2000) Induction of neurogenesis in the neocortex of adult mice. Nature 405:951–955.

Menezes JR, Luskin MB (1994) Expression of neuron-specific tubulin defines a novel population in the proliferative layers of the developing telencephalon. J Neurosci 14:5399–5416.

Menezes JR, Smith CM, Nelson KC, Luskin MB (1995) The division of neuronal progenitor cells during migration in the neonatal mammalian forebrain. Mol Cell Neurosci 6:496–508.

Michel R, Cruz-Orive L (1988) Application of the Cavalieri principle and vertical sections method to lung: estimation of volume and pleural surface area. J Microsc 150:117–136.

Mizisin A, Bache M, DiStefano P, Acheson A, Lindsay R, Calcutt N (1997) BDNF attenuates functional and structural disorders in nerves of galactose-fed rats. J Neuropathol Exp Neurol 56:1290–1301.

Morgan R, Couture L, Elroy-Stein O, Ragheb J, Moss B, Anderson WF (1992) Retroviral vectors containing putative internal ribosomal entry sites: development of a polycistronic gene transfer system and applications to human gene therapy. Nucleic Acids Res 20:1293–1299.

Palmer T, Markakis E, Willhoite A, Safar F, Gage F (1999) FGF-2 activates a latent neurogenic program in neural stem cells from diverse regions of the adult CNS. J Neurosci 19:8487–8497.

Palmer TD, Ray J, Gage FH (1995) FGF-2-responsive neuronal progenitors reside in proliferative and quiescent regions of the adult rodent brain. Mol Cell Neurosci 6:474–486.

Paxinos G, Watson C (1986) The rat brain in stereotaxic coordinates, Ed. 2. Orlando, FL: Academic.

Pelleymounter M, Cullen M, Wellman C (1995) Characteristics of BDNF-induced weight loss. Exp Neurol 131:229–238.

Pencea V, Bingaman K, Wiegand S, Luskin M (1999) Infusion of BDNF into the lateral ventricle of the adult rat leads to an increase in the number of newly generated cells in the fore-, mid- and hindbrain parenchyma. Soc Neurosci Abstr 25:2045.

Pincus D, Harrison C, Goodman R, Edgar M, Keyoung HM, Fraser R, Nedergaard M, Goldman SA (1998) FGF2/BDNF-associated maturation of new neurons generated from adult human subependymal cells. Ann Neurol 43:576–585.

Reynolds BA, Weiss S (1992) Generation of neurons and astrocytes from isolated cells of the adult mammalian central nervous system. Science 255:1707–1710.

Richards LJ, Kilpatrick TJ, Bartlett PF (1992) De novo generation of neuronal cells from the adult mouse brain. Proc Natl Acad Sci USA 89:8591–8595.

Roy N, Wang S, Benraiss A, Fraser R, Gravel P, Braun P, Goldman S (1999) Identification, isolation and enrichment of oligodendrocyte progenitor cells from the adult human subcortical white matter. J Neurosci 19:9986–9995.

Roy N, Wang S, Jiang L, Kang J, Restelli C, Fraser R, Couldwell W, Kawaguchi A, Okano H, Nedergaard M, Goldman SA (2000) In vitro neurogenesis by neural progenitor cells isolated from the adult human hippocampus. Nat Med 6:271–277.

Sterio D (1984) The unbiased estimation of number and sizes of arbitrary particles using the dissector. J Microsc 134:127–136.

Vescovi AL, Reynolds BA, Fraser DD, Weiss S (1993) bFGF regulates the proliferative fate of unipotent (neuronal) and bipotent (neuronal/astroglial) EGF-generated CNS progenitor cells. Neuron 11:951–966.

Waldvogel H, Faull R, Dragunow M (1991) Differential sensitivity of calbindin and parvalbumin immunoreactive cells in the striatum to excitotoxins. Brain Res 546:329–335.

Wang Y, Sheen V, Macklis J (1998) Cortical interneurons upregulate neurotrophins in vivo in response to targeted apoptotic degeneration of neighboring pyramidal neurons. Exp Neurol 154:389–402.

West M (1998) Stereological methods for estimating the total number of neurons and synapses: issues of precision and bias. Trends Neurosci 22:51–61.

Yoon S, Lois C, Alvirez M, Alvarez-Buylla A, Falck-Pedersen E, Chao M (1996) Adenovirus-mediated gene delivery into neuronal precursors of the adult mouse brain. Proc Natl Acad Sci USA 93:11974–11979.

Zigova T, Peneca V, Wiegand S, Luskin M (1998) Intraventricular administration of BDNF increases the number of newly generated neurons in the adult olfactory bulb. Mol Cell Neurosci 11:234–245.